ELSEVIER

Journal of Structural Geology 28 (2006) 1670–1684

JOURNAL OF STRUCTURAL GEOLOGY

www.elsevier.com/locate/jsg

The structure and kinematics of an imbricate stack of oceanic rocks in the Jurassic accretionary complex of Central Japan: an oblique subduction model

Masakazu Niwa*

Division of Earth and Environmental Sciences, Graduate School of Environmental Studies, Nagoya University, Nagoya, 464-8602 Japan

Received 22 November 2005; received in revised form 19 June 2006; accepted 20 June 2006
Available online 23 August 2006

Abstract

The Jurassic accretionary complex of the Mino Belt in the Takayama area, Central Japan includes a major unit characterized by abundant bedded chert and basalt slabs. This unit has an imbricate structure, represented by the repetition of stratigraphic layers composed of sandstone, black mudstone, felsic tuff, bedded chert, siliceous claystone, limestone and basalts. Shear zones subparallel to the trend of the slabs occur in the siliceous claystones and basalts. Deformation structures in the shear zones suggest that phyllosilicate-rich layers within the accretionary complex were preferentially weakened due to grain size reduction by cataclasis and pressure solution-accommodated deformation. Restored shear directions in the siliceous claystones and basalts indicate dextral kinematics subparallel to the trench axis. In contrast, mesoscopic asymmetric folding of the bedded chert, indicated from the restored shear, was oblique or normal to the trench axis. To interpret the two distinct shear directions, a model is proposed in which the constituent rocks of this unit were obliquely subducted dextrally along the East Asian continental margin. Due to the oblique subduction, slip vectors were apparently partitioned into trench-orthogonal components in the shallower part of the subduction zone and trench-parallel components in the deeper part.

Keywords: Kinematic analysis; Imbricate structure; Oceanic rocks; Accretionary complex; Transpression; Central Japan

1. Introduction

The formation of accretionary complexes is one of the most common geological processes in subduction zones. Accretionary complexes preserve, in their lithologic and structural makeup, detailed records of the deformation that occurred in subduction zones. Their constituent rocks typically comprise the upper part of the oceanic crust, consisting of basalts with the overlying sedimentary rocks. Accreted sedimentary rocks along plate margins often develop imbricate structures at the outcrop and map scales due to thrusting and shearing, and can develop block-in-matrix fabric at the outcrop scale due to the deformation induced by layer-parallel extension and shearing. Many studies have focused on kinematic analyses of accreted sedimentary rocks from the Pacific coast of North America (e.g. Cowan, 1985; Sample and Moore, 1987; Orange, 1990; Kusky et al., 1997), Italy (e.g. Pini, 1999; Bettelli and Vannucchi, 2003), Japan (e.g. Kano et al., 1990; Kimura and Mukai, 1991; Kimura and Hori, 1993; Ujiie, 2002) and elsewhere (e.g. Platt et al., 1988; Kano and Konishi, 2001). In addition, the accretion and exhumation of oceanic crust has also been discussed (e.g. Kimura and Ludden, 1995; Kusky and Young, 1999; Ueda et al., 2000; Kusky et al., 2004). However, detailed kinematic analyses of accreted oceanic crust are still rare. Although drill cores from modern subduction zones provide useful information for understanding the formation and deformation of accretionary complexes as well as uplifted ancient accretionary complexes (e.g. Maltman et al., 1993; Labaume et al., 1997), well-preserved drill cores

* Present address: Tono Geoscientific Research Unit, Japan Atomic Energy Agency, 959-31, Jorinji, Izumi, Toki, Gifu 509-5102, Japan. Tel.: +81 572 53 0211; fax: +81 572 55 0180.
E-mail address: niwa.masakazu@jaea.go.jp

0191-8141/$ - see front matter © 2006 Elsevier Ltd. All rights reserved.
doi:10.1016/j.jsg.2006.06.011

that include intensely sheared rock derived from oceanic crust have yet to be obtained successfully. Therefore it is instructive to describe the deformation structures preserved in the oceanic crust within uplifted ancient accretionary complexes for elucidating further details about accretion and exhumation processes.

This paper provides a description and analysis of the structures, kinematics and deformation of the imbricate stack of oceanic rocks located in the Takayama area of Central Japan, where a Jurassic accretionary complex of the Mino Belt is exposed. Regionally, the Mino Belt is composed predominantly of accretionary complexes of Jurassic to Early Cretaceous age (e.g. Otsuka, 1988; Wakita, 1988; Fig. 1). The belt includes an abundance of accreted oceanic rocks such as bedded chert, limestone and basalts. Although several workers have discussed the accretion of the oceanic rocks (e.g. Okamura, 1991), there are few studies of the Mino Belt describing in detail the deformation structures.

2. Regional setting

The Mino Belt in Central Japan includes Jurassic to Early Cretaceous accretionary complexes. A Middle Jurassic accretionary complex of the Mino Belt outcrops in the Takayama area. The exposure is about 13 km north to south and about 24 km east to west and is located approximately 300 km west of Tokyo (Adachi and Kojima, 1983; Kojima, 1984; Yamada et al., 1985; Figs. 1 and 2).

The Jurassic accretionary complexes of the Mino Belt in Central Japan are roughly divided into two major lithostratigraphic units based on their field occurrence: a coherent unit and a melange unit (Isozaki, 1997a). The coherent unit is composed of imbricate thrust sheets, each of which partly preserves primary stratigraphic relationships. This major unit is subdivided based on the dominant rock types into a chert-basalt unit and a clastic rock unit. In contrast, the melange unit is composed of mixed rock assemblages, including various sized clasts derived from the various constituent rocks of the accreted rocks in a mudstone matrix.

In the Takayama area, the Mino Belt is also subdivided into the same major rock units outlined above: the coherent unit, which is subdivided into a chert-basalt unit and a clastic rock unit, and the melange unit, which for the purpose of this study, has not been subdivided (Niwa, 2004; Fig. 2). The coherent chert-basalt unit is comprised of imbricate slabs of bedded chert, basalts, sandstone, black mudstone, felsic tuff, siliceous claystone and limestone. The coherent clastic rock unit is comprised of alternating beds of sandstone and mudstone interbedded with a minor felsic tuff and bedded chert. The melange unit includes clasts of sandstone, felsic tuff, bedded chert, siliceous claystone, limestone and basalts set in a matrix of mudstone. The chert-basalt, the clastic rock and the melange units occur in thrust fault contact with each other. The thrust faults are generally oblique (locally parallel) to local bedding planes and to the preferred alignment of the imbricate slabs in the coherent chert-basalt unit.

The rocks of the Mino Belt in the Takayama area form a synclinorium with a west-southwest plunging axis (Fig. 2). The half-wavelength of the largest synclinal fold is at least several kilometers. The axis of the synclinal fold trends S76°W and plunges 35°W. The bedding planes in the southern limb of the syncline strike northeast to east-northeast and dip steeply north to northwest, while the bedding planes in the northern limb strike west-northwest to east-northeast with southerly dips.

This paper is focused on structural and kinematic analysis of the coherent chert-basalt unit preserved in the southern limb of the largest synclinal fold in the study area in order to develop an understanding of the deformation and kinematics of the oceanic rocks during accretion.

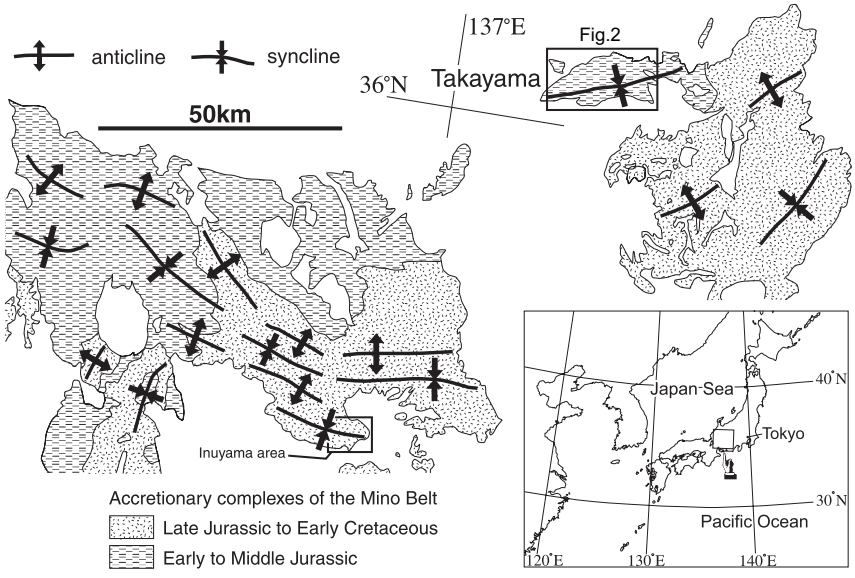

Fig. 1. Index map showing the location of the Takayama area and the exposure of accretionary complexes of the Mino Belt, Central Japan (modified from Nakae, 2000).

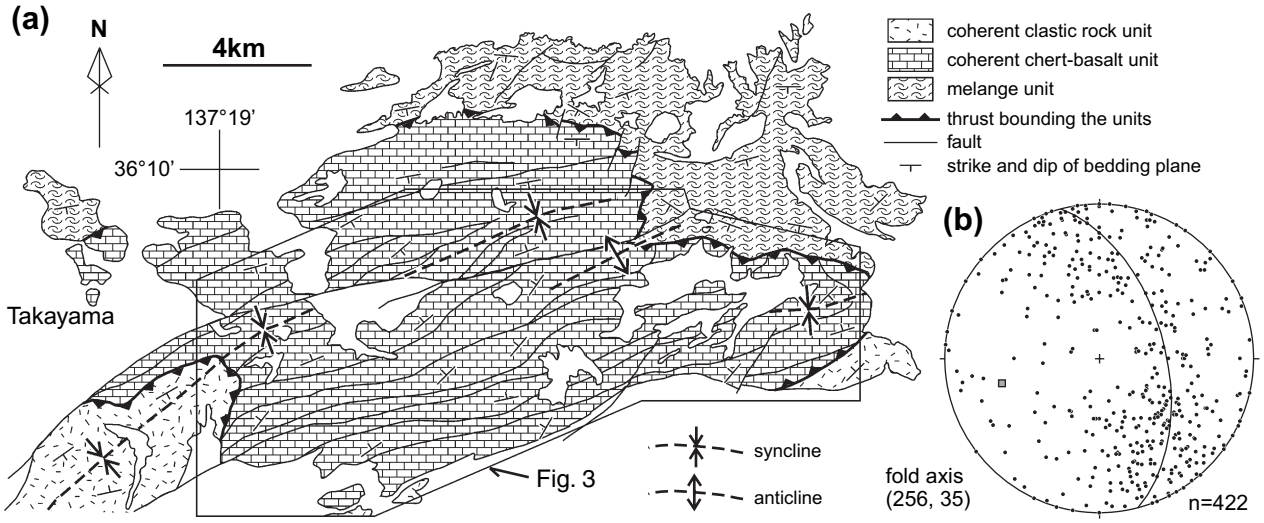

Fig. 2. (a) Simplified geological map of the Takayama area (modified from Niwa, 2004), showing Middle Jurassic accretionary complexes. See Fig. 1 for location. (b) Equal-area lower hemisphere projection of poles to bedding planes in the coherent chert-basalt unit. Square shows trend and plunge of the regional fold axis.

The constituent rocks of the Mino Belt are a complex assemblage of distinct rock types as follows: basalts derived from seamounts mainly formed near oceanic ridges; overlying marine sedimentary rocks such as bedded radiolarian chert and pelagic limestone; and trench-fill terrigenous clastic rocks such as felsic tuff, mudstone and sandstone (Isozaki, 1997a). The primary 'oceanic plate stratigraphy' prior to accretion can be reconstructed based on microfossil evidence and lithologic features (Matsuda and Isozaki, 1991; Isozaki, 1996, 1997a). This stratigraphy consists of a Permian basalt-limestone-chert sequence, latest Permian to Early Triassic siliceous claystone, Middle Triassic to Middle Jurassic radiolarian chert and Early Jurassic to Late Jurassic felsic tuff, black mudstone and sandstone (Wakita and Metcalfe, 2005).

In the coherent chert-basalt unit of the Takayama area, radiolarians in the bedded chert and felsic tuff indicate Permian to Early Jurassic and Middle Jurassic ages, respectively (Kojima, 1982, 1984; Adachi and Kojima, 1983; Imazato and Otoh, 1993). Limestones in this area contain Permian fusulinoideans (Kojima, 1984; Adachi and Kojima, 1983). On the basis of the previously reported microfossil data, the stratigraphy in the study area has been reconstructed. It is composed of a Permian basalt-limestone-chert sequence, latest Permian to Early Triassic siliceous claystone, Middle Triassic to Early Jurassic radiolarian chert and Middle Jurassic felsic tuff, black mudstone and sandstone, in ascending order. The overall outcrop pattern in the coherent chert-basalt unit appears to repeat partial or complete packages of preserved oceanic plate stratigraphy, though original depositional contacts between each lithology are rarely preserved due to the effects of later shearing.

In the Takayama area, each slab of bedded chert and basalts in the coherent chert-basalt unit is several hundred meters to tens of kilometers in length and several tens to hundreds of meters in thickness. The slabs extend in ENE-WSW, subparallel to the regional trend of the bedding. Field mapping shows that the rocks of the coherent chert-basalt unit have the form of imbricate thrust sheets (Fig. 3).

3. Deformation structures in the coherent chert-basalt unit

In the coherent chert-basalt unit of the Takayama area, two types of structure due to deformation of oceanic rocks have been identified: shear zones and mesoscopic asymmetric folds. The folds typically affect the bedded cherts, whilst the shear zones occur preferentially along the siliceous claystones and along the bases of the basalt slabs where they represent imbricate thrust faults. Widths of the shear zones range from several meters to tens of meters. The shear zones are characterized by a block-in-matrix fabric and have developed an intense foliation. The trend of the shear zones is subparallel to each lithology in the coherent chert-basalt unit. The bedded chert is, in part, asymmetrically folded with half-wavelengths of several meters, although the enveloping surface of the folds is subparallel to an alignment of the slabs in a regional sense.

In the following section, the deformation structures formed by shearing of oceanic rocks are described in more detail.

3.1. Deformation structures

3.1.1. Shear zones in the siliceous claystone

Siliceous claystones in this area comprise rhythmical alternating beds of grey siliceous rock and black claystone (Fig. 4a,b). The grey siliceous rocks include abundant siliceous spherical shells derived from radiolarian fossils, accompanied by fine grains of quartz and clay minerals. The black claystones are composed mainly of fine dark grains of clay and opaque minerals. Euhedral grains of pyrite are abundant (Fig. 4a). No clastic grains larger than silt-size are present except for radiolarian fossils and pyrite grains. Based on the

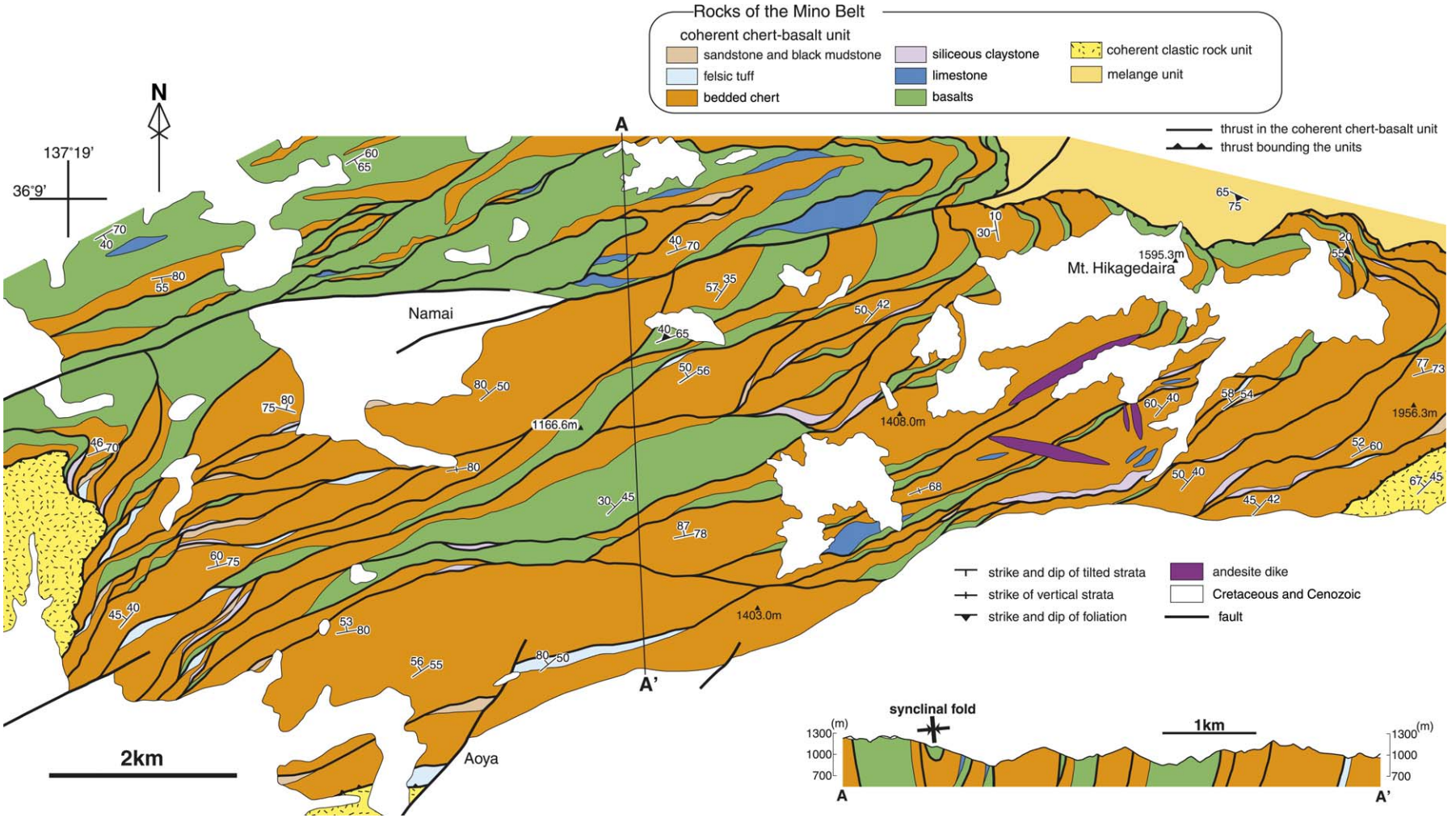

Fig. 3. Geological map and cross section showing the lithologies and general structure in the coherent chert-basalt unit. See Fig. 2 for location.

observed mesoscopic and microscopic characteristics, the siliceous claystone is considered to be a ''Toishi''-type siliceous claystone. This is the key bed indicative of a Lower Triassic origin that typically occurs just above the Permian/Triassic boundary in bedded chert sequences in the Jurassic accretionary complexes in Japan (e.g. Imoto, 1984; Isozaki, 1997a,b; Suzuki et al., 1998).

Most parts of the siliceous claystone show intense deformation by layer-parallel extension and shearing (Fig. 4b). The grey siliceous component of the sheared siliceous claystone shows pinch-and-swell structures or boudinage, and has an irregular contact with the black claystone component. Riedel (R1) shears (Logan et al., 1979; Rutter et al., 1986) crosscut the primary bedding of the sheared siliceous claystone (Fig. 4b). The rocks of the grey siliceous beds are broken into lenticular or irregularly shaped clasts in the black claystone matrix. The lenticular clasts have elongated tails formed from the same materials as the clasts and occur with a preferred alignment. The fine-grained clay minerals in the matrix are aligned subparallel to the alignment of the lenticular clasts. The alignment of the clay minerals and lenticular clasts defines a P foliation. In many cases, the P foliation lies at a shallow angle to the Y shears, which correspond to the principal displacement shear surface. Pressure solution cleavages of thin dark fine-grained layers are roughly arranged along the Y shear in the black claystone (Fig. 4c). Opaque minerals in the black claystone are associated with pressure shadows or pressure fringes.

Veins, mainly filled with quartz, occur in the lenticular clasts of the grey siliceous rock. The veins intersect the clasts at a high angle to their preferred orientation, but do not extend into the matrix (Fig. 4c).

The grey siliceous rocks typically have patterned, indented surfaces with depressions filled with a dark fine-grained matrix material (Fig. 4d). Several depressions are rounded. The fine, dark grains are considered to by dissolution and precipitation during fluid-assisted diffusive mass transfer. The precipitated grains are laminated as a result of growing concentrically around the rounded rims of the depressions.

3.1.2. Shear zones in the basalts

Basalts in this area are composed of pillow or massive basalt lavas and basaltic volcaniclastic rocks. The basalt lavas are typically green or red, composed of clinopyroxene and plagioclase with secondary chlorite, sericite, pumpellyite, calcite and opaque minerals. The basaltic volcaniclastic rocks consist of tuff breccia and tuff interbedded subparallel to the imbricate slabs. They include crystals of plagioclase with secondary chlorite, sericite, illite, muscovite, pumpellyite, calcite, quartz and opaque minerals. The basalts exhibit very low-grade metamorphism equivalent to the prehnite-pumpellyite facies.

The shear zones preferentially formed along the basal part of the basalt slabs (Fig. 4e–h). The shear zones include lenticular or oval clasts of chert, basalt lava and basaltic tuff breccia set in a matrix of fine fragments and secondary minerals. The P foliation is defined by a strong alignment of phyllosilicates such as sericite, chlorite, illite and muscovite in the matrix (Fig. 4f,g). The P foliation is finely laminated, with laminations having a spacing of less than 0.1 mm. The clasts in the shear zones are wrapped by the matrix phyllosilicates, and are preferentially arranged along the P foliation. Several phyllosilicate-bearing clasts are accompanied by elongated tails or pressure shadows. The tails are fine-grained, composed of the same material as the clasts. The pressure shadows are derived from dissolved and precipitated matrix phyllosilicates. Pressure solution cleavages of thin, fine dark layers are developed in a manner similar to the composite planar fabric of the Y shears and Riedel (R1) shears elsewhere in the sequence.

3.1.3. Mesoscopic folding of bedded chert

Asymmetric mesoscopic folds are the most visible deformation structure in the bedded chert. In parts of the bedded chert slabs, chert layers are deformed into chevron or kink folds. The half-wavelength and amplitude of the folds range from several tens of centimeters to meters. When the interlimb angle is acute, the folds have asymmetric shapes similar to the S-shaped or Z-shaped folds described by Otsuka (1989) (Fig. 5). Otherwise, the folds show kink geometries with larger interlimb angle (more than 90°).

Chert layers are abruptly but smoothly bent in the hinges. The hinges are sharp and the limbs are planar or slightly undulating. Remarkably, cataclasis is not observed in the folded bedded chert, although tension cracks filled with quartz are widespread developed normal to the layering. Chert layers are slightly thickened at the hinges. Radiolarian shells in the chert are not flattened significantly, though the fold limbs are slightly deformed into pinch-and-swell structures due to layer-parallel extension during folding. Based on the fold geometry and asymmetry, the folds are considered to have been formed by drag induced by thrust-related shearing along the chert layers.

3.2. Shear sense indicators

Penetrative shear zones are well developed in the siliceous claystones and basalts of the coherent chert-basalt unit. Composite planar fabrics related to the P foliation, Y shears and R1 shears can be identified in the shear zones. The P foliation is defined by the preferred alignment of the fine-grained phyllosilicates and lenticular clasts in the matrix, and lies at a shallow angle to local bedding. The Y shears corresponds to the principal displacement shear surfaces, and lie mostly subparallel to bedding and to the trend of the shear zones. The Y shear runs in an orientation between 10° and 30° to the P foliation. The R1 shears are defined by thin layers of very fine-grained materials, intersecting the Y shears at 10° to 45°. In the southern limb of the synclinal fold of the coherent chert-basalt unit in the Takayama area, the Y shears strike east to northeast and dip north (locally dipping steeply south). The composite planar fabric is exactly analogous to the argillite-matrix melange fabric described by Kusky and Bradley (1999) in the accretionary complex of Alaska.

In this study, the following asymmetric fabric elements are used for kinematic analysis of the shear zones: (1) Obliquity of

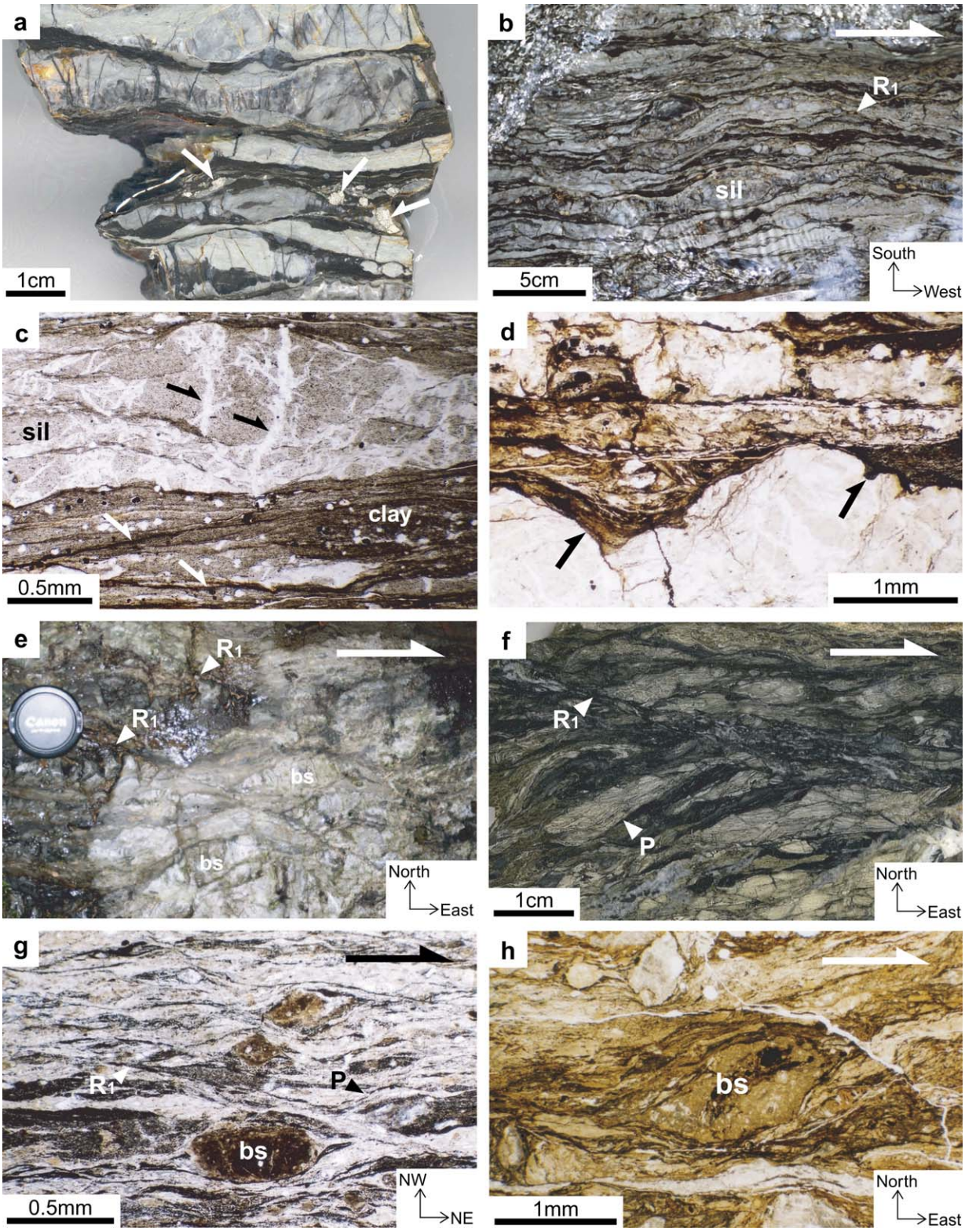

Fig. 4. Photographs and photomicrographs showing deformation structures in the siliceous claystone and basalts. (a) Polished surface of sheared siliceous claystone showing boudinage. Secondary pyrite is abundant in the black claystone (white arrows). (b) Field occurrence of ductilely sheared siliceous claystone. The grey siliceous component (sil) shows boudinage with a dextral sense of shear (white arrow). The dextral R1 shear cuts the boudins. (c) Photomicrograph showing quartz veins (black arrows) in the grey siliceous component (sil) and pressure solution cleavage (white arrows) in the black claystone (clay) of the siliceous claystone (plane polarized light). (d) Photomicrograph showing patterned indented surface of the grey siliceous component of the siliceous claystone (plane polarized light). The depressions are rounded and filled with dark fine-grained matrix material (black arrows). The dark fine grains are laminated as a result of growing concentrically along the rounded rims of the depressions. (e) Field occurrence of sheared basalts. The R1 shears and sigma-type basalt lenses (bs) indicate dextral shear (white arrow). (f) Polished surface of sheared basalts. The R1 shear cuts the P foliation defined by strong alignment of phyllosilicates, indicating dextral shear (white arrow). (g) Photomicrograph of sheared basalts (plane polarized light). Sigma-type basalt clast (bs) with associated pressure shadows indicating dextral shear (black arrow). The dextral R1 shear cuts the P foliation. (h) Photomicrograph showing lenticular basalt clast (bs) with asymmetric tails (plane polarized light). The sigma-type shape indicates dextral shear (white arrow).

the P foliation or R1 shear with respect to the Y shears (e.g. Takagi, 1996; Fig. 4b,e–g); and (2) asymmetric shapes of the lenticular clasts with tails, pressure shadows or pressure fringes showing sigma or delta shapes (e.g. Passchier and Trouw, 1996; Fig. 4b,e,g,h).

Shear directions were determined using the asymmetric fabric elements and the orientation of the intersection lineation between the Y shears, P foliation or R1 shears. In the latter case, the direction in the plane of the Y shear and perpendicular to the intersection lineation is the shear direction. In many cases, the long axes of lenticular clasts are oriented subparallel to the shear direction determined by the intersection lineation. Slickenlines, which are defined by linear grooves formed by an orderly alignment of phyllosilicates developed on the surfaces of the P foliations and Y shears. Slickenline lineations are typically oriented subparallel to the long axes of lenticular clasts, which supports the above observation that the long axes of the lenticular clasts are subparallel to the shear direction.

In the shear zones of the siliceous claystones and basalts, the shear direction deduced is, for the most part, dextral strike-slip and reverse dip-slip, i.e. top-to-the-east, for a shear plane with a northeast strike and northwesterly dip (Figs. 6 and 7, Table 1).

Asymmetric mesoscopic folds in the bedded chert, i.e. the S-shaped and Z-shaped folds and kink folds, are another potential indicator of shear direction (Fig. 5). The direction normal to the hinge line and parallel to the fold envelope plane corresponds to the shear direction of the folds. In the present study, the shear directions indicated by asymmetric mesoscopic folds in the bedded chert lie on the southern limb of the map-scale synclinal fold of the coherent chert-basalt unit and are predominantly top-to-the-south or -southeast (Figs. 6 and 7, Table 2).

4. Discussion

4.1. Preferred decollement zones in the oceanic imbricate stack and weakening of basalts

In the coherent chert-basalt unit, shear zones occur preferentially in the siliceous claystones and basalts. The preferential development of decollements in the "Toishi"-type siliceous claystones is also observed in other studies of imbricate stacks composed of chert and clastic rocks in the Jurassic accretionary complex of Japan (e.g. Kimura and Hori, 1993; Nakae, 1993). The siliceous claystones have abundant fine-grained phyllosilicates that define a well-developed foliation. Aligned phyllosilicates are considered to have had a significant influence on the rock strength with respect to shearing, in particular under conditions favoring pressure solution (e.g. Bos and Spiers, 2001).

In general, the brittle-ductile transition zone for phyllosilicate-bearing fault rocks can occur across a broad depth range from 5 to 20 km (e.g. Bos and Spiers, 2002; Jefferies et al., 2006) with temperature conditions in subduction zones typically lying in the range of 75 to 300 °C and differential stresses of 40 to 80 MPa. The rocks of the coherent chert-basalt unit in the Takayama area are metamorphosed to the prehnite-pumpellyite facies. The P/T conditions under which prehnite-pumpellyite facies typically develops occurs wholly within the brittle-ductile transition zone for phyllosilicate-bearing fault rocks in subduction zones (Liou et al., 1987).

Grain-size reduction by cataclasis can lead to enhanced development of phyllosilicate minerals under hydrothermal conditions equivalent to the brittle-ductile transition zone (Janecke and Evans, 1988; Wintsch et al., 1995). Such phyllosilicate minerals produced under these conditions are believed to increase grain boundary diffusion rates, enhancing diffusional mass transfer processes and further foliation development (Means and Williams, 1972; Renard et al., 1997; Farver and Yund, 1999; Collettini and Holdsworth, 2004; Jefferies et al., 2006). Following the experimental finding of Bos and Spiers (2002), it seems likely that subduction to the depth of the brittle-ductile transition zone, grain-size reduction by cataclasis and subsequent formation of fine-grained phyllosilicates and development of the foliation due to pressure solution-accommodated deformation of the fine-grained phyllosilicates probably induced weakening of the siliceous claystones and accommodated thrusting within slabs of the coherent chert-basalt unit.

It is important to note that many shear zones also formed preferentially in the basalts. Phyllosilicates such as chlorite and sericite are also abundant in the basalts and are derived from altered clinopyroxene and plagioclase, respectively. Finely laminated foliation, defined by a strong alignment of phyllosilicates, is developed in the phyllosilicate-bearing basalts. Accordingly, pressure solution probably accommodated the deformation in the phyllosilicate-bearing basalts as well as the siliceous claystones. Progressive fracturing, subsequent cataclasis, and alteration to phyllosilicates transformed massive basalts into mica phyllonites within shear zones that are tens of meters wide, as described elsewhere by Janecke and Evans (1988), and Jefferies et al. (2006). Wintsch et al. (1995) suggest that phyllosilicates are expected to form in deformed mafic rocks that are more Mg rich compared to deformed granites. The deformation structure of the basalts in the study area suggests that the basalts are weakened due to grain size reduction by cataclasis and pressure solution-accommodated deformation within the brittle-ductile transition zone in the subduction zone setting. The phyllosilicate-bearing siliceous claystones and basalts are therefore most likely to form the preferred decollements along which the imbricate structures of the coherent chert-basalt unit were localized.

In contrast, penetrative shear zones equivalent to the decollements do not occur within the bedded cherts and limestones, probably because these rocks lack the fine-grained phyllosilicates that accelerated the weakening and shearing in the siliceous claystones and basalts.

Mesoscopic folding of bedded cherts is common in accretionary complexes (e.g. Brueckner and Snyder, 1985; Otsuka, 1989; Kimura and Hori, 1993; Kusky and Bradley, 1999). The transformation from opal-A through opal-CT to quartz

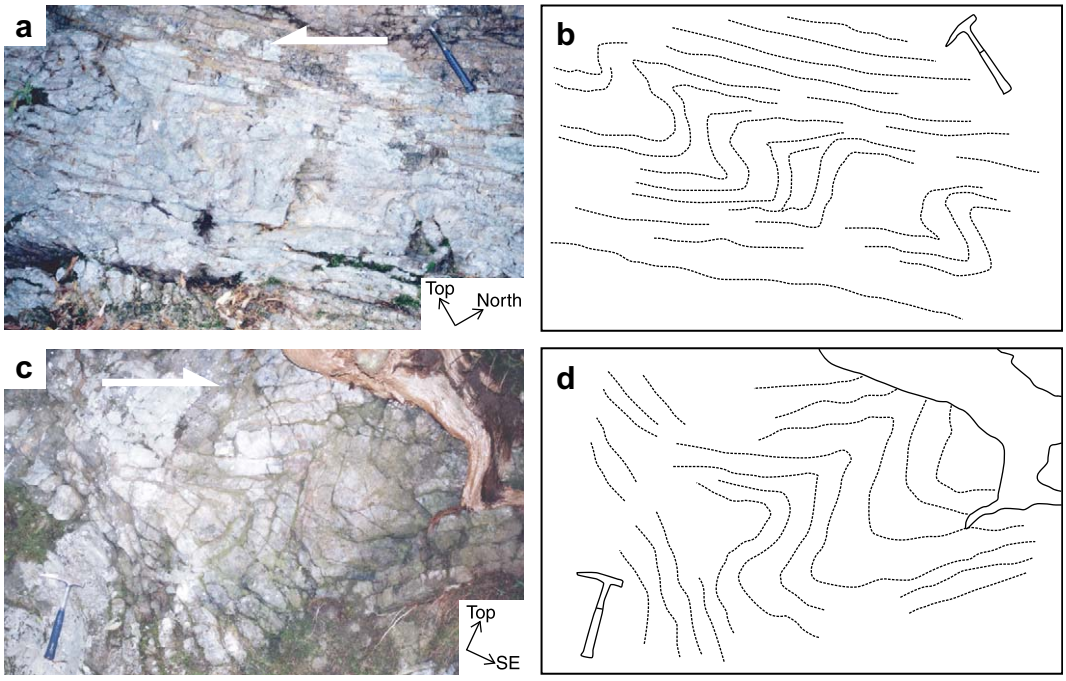

Fig. 5. Photographs showing deformation structures in bedded chert. (a and b) Field occurrence and sketch showing an "S-shaped" fold of bedded chert which indicates reverse dip-slip sense of shear (white arrow). (c and d) Field occurrence and sketch showing a "Z-shaped" fold of bedded chert which indicates reverse dip-slip sense of shear (white arrow).

results in major changes in the mechanical properties of chert (Williams et al., 1985). The mesoscopic features of folds in chert are likely linked to the changing silica-diagenetic conditions during folding (Brueckner et al., 1987). In the coherent chert-basalt unit of the Takayama area, the thickening of chert layers in the hinges of the folds and the lack of flattened radiolarian shells indicate that the chert was soft enough to permit inter-granular flow during folding, though the chert layers were competent enough to undergo initial buckling. The silica-diagenetic conditions associated with the opal-CT transformation are most favorable for the formation of the mesoscopic folding (Brueckner et al., 1987; Kimura and Hori, 1993). This suggests that the mesoscopic folding is unlikely to have occurred due to the development of flexural-slip folds at a post-accretion stage formed due to bedding-parallel slip during the synclinal folding with a west-southwest plunging axis in the Takayama area.

The temperature of the transformation of opal-CT to quartz in the sedimentary realm is considered to lie within the range of 31 to 165 °C (e.g. Williams and Crerar, 1985) or less than 100 °C (Behl and Garrison, 1994). Deformation by diffusive mass transfer, which is involved with shearing in the phyllosilicate-rich rocks, starts at 100 to 120 °C and peaks at over 200 °C (Moore and Allwardt, 1980; DiTullio and Byrne, 1990; Fisher and Byrne, 1992; Moore and Saffer, 2001). Accordingly, it is suggested that the mesoscopic asymmetric folding of the bedded chert occurred at lower temperatures in the shallower part of the subduction zone prior to much of the shearing in the siliceous claystones and basalts.

4.2. Are restored shear directions parallel to plate motions?

In accretionary complexes with preserved imbricate thrust sheets, several workers have suggested that the slip directions recorded by each thrust should correspond directly to the subducted plate motions reconstructed by paleomagnetic studies and hotspot track analyses (e.g. Kano et al., 1990; Kimura and Mukai, 1991; Kimura, 1999; Kusky and Bradley, 1999). Mesoscopic asymmetric folding of bedded chert is also suggested to indicate the same shear direction as the thrusts (Otsuka, 1989; Kimura and Hori, 1993; Kimura, 1997, 1999). However, in the present study, the shear directions are clearly different for the mesoscopic folding of the bedded cherts compared to those recorded by the thrust shear zones in the siliceous claystones and basalts in the coherent chert-basalt unit of the Takayama area (Figs. 6 and 7). The folds record predominantly top-to-the-south to top-to-the-southeast senses, whilst the shear zones in the siliceous claystones and basalts indicate top-to-the-east movements.

Kimura and Hori (1993) and Kimura (1997, 1999) examined the thrust shear direction after correction/restoration of regional folding, tilting and rotation in the imbricate stack composed of clastic rocks and bedded cherts in the Late Jurassic accretionary complex of the Mino Belt of the Inuyama area (Fig. 1). First, the shear direction was rotated counterclockwise around a vertical axis and restored to the position before the Miocene rotation of Southwest Japan, which is involved with the opening of the Japan Sea (Otofuji et al., 1985; Jolivet et al., 1994) and the collision of the Izu-Bonin Arc with the

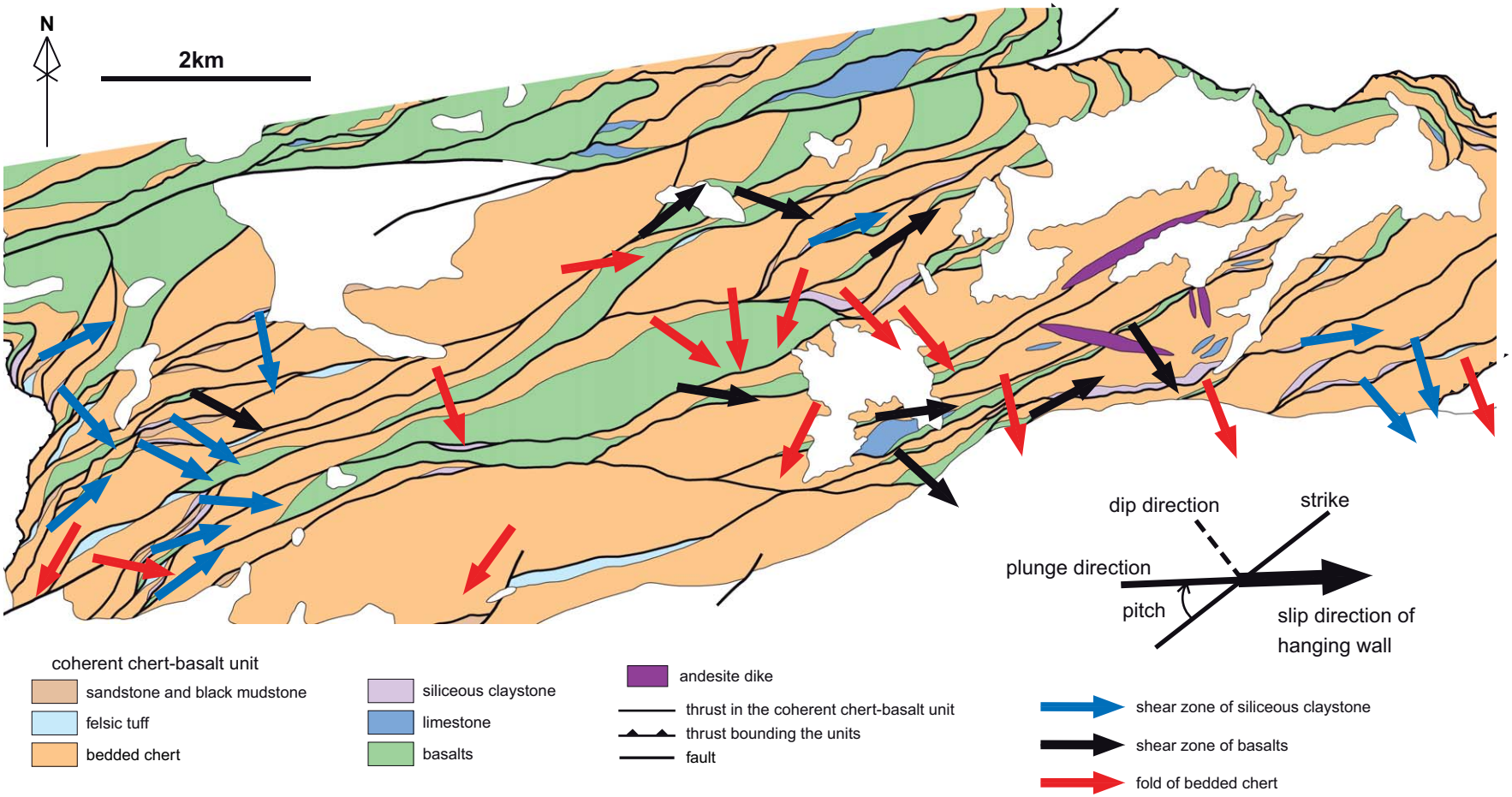

Fig. 6. Shear directions on the northern side of shear zone planes in the siliceous claystone and basalts, and the asymmetric folds in bedded chert, traced on the geological map.

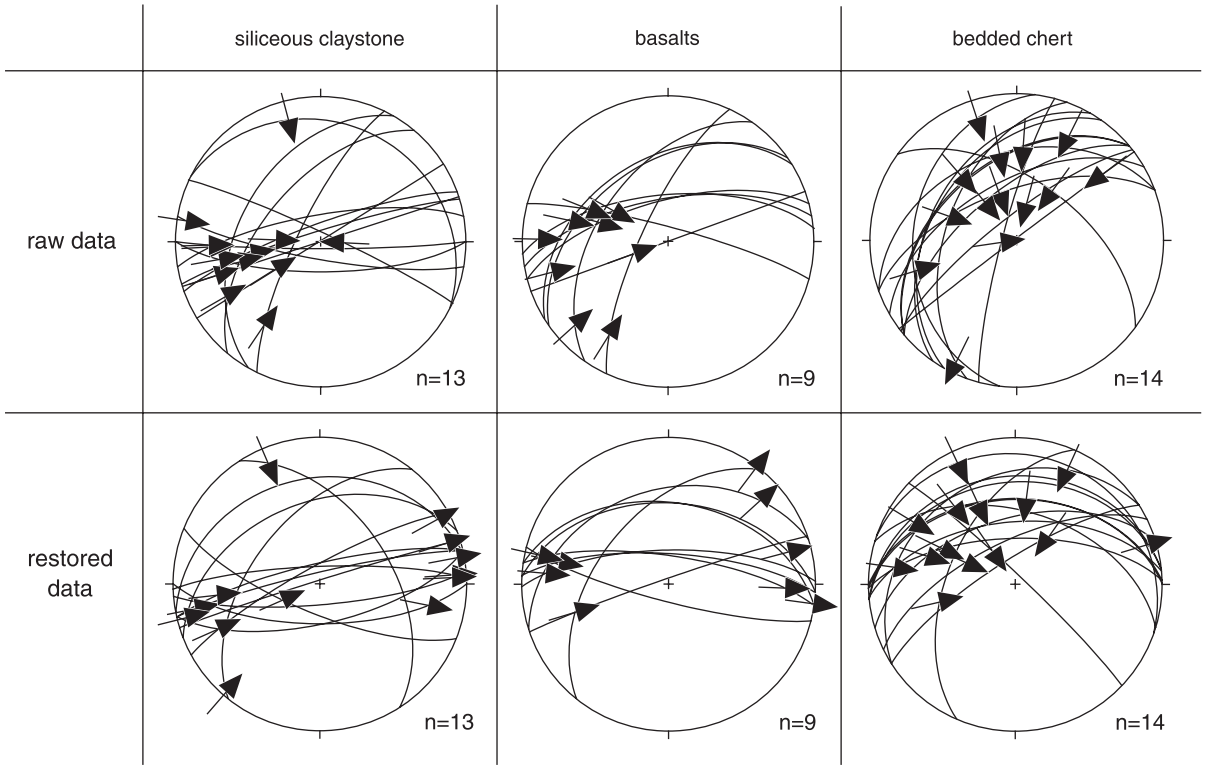

Fig. 7. Equal-area lower hemisphere projections showing shear directions of the shear zones of siliceous claystone and basalts, and the asymmetric folds of bedded chert, before and after the restoration of tilting associated with the synclinal fold with a west-plunging axis. Black arrows indicate the directions on the northern side of Y shear planes. All data were collected from the southern limb of the synclinal fold.

Table 1
Structural data from the shear zones of siliceous claystone and basalts

Raw data		Restored data		
Y shear	Kinematic indicator	Y shear	Shear direction	Pitch
Siliceous claystone				
(342, 90)	Slickenline (252, 25)	(343, 88)	(72, 10)	−10
(350, 75)	Slickenline (267, 25)	(356, 80)	(86, 9)	−10
(179, 75)	R1 shear (195, 85)	(167, 68)	(80, 5)	−5
(180, 86)	P foliation (157, 77)	(175, 79)	(87, 10)	−11
(190, 80)	R1 shear (211, 83)	(180, 68)	(101, 25)	−27
(328, 90)	Slickenline (238, 60)	(331, 80)	(246, 26)	26
(343, 84)	Slickenline (260, 50)	(347, 83)	(258, 15)	15
(297, 76)	P foliation (283, 84)	(308, 52)	(221,3)	4
(340, 80)	Slickenline (272, 65)	(347, 78)	(264, 31)	31
(300, 43)	Slickenline (240, 25)	(348, 28)	(61, 9)	−19
(310, 58)	R1 shear (321, 49)	(338, 43)	(256, 7)	10
(25, 85)	R1 shear (19, 60)	(202, 73)	(246, 67)	74
(27, 19)	P foliation (5, 37)	(57, 49)	(337, 12)	16
Basalts				
(331,45)	R1 shear (17, 30)	(8, 43)	(98, 0)	0
(295, 75)	R1 shear (321, 63)	(309, 50)	(37, 2)	−2
(345, 67)	Slickenline (285, 50)	(359, 70)	(275, 18)	19
(350, 66)	Slickenline (299, 55)	(3, 73)	(282, 26)	27
(340, 90)	Slickenline (250, 70)	(341, 87)	(254, 35)	35
(325, 45)	P foliation (297, 62)	(3, 44)	(75, 16)	−24
(15, 82)	R1 shear (30,70)	(195, 81)	(283, 11)	11
(305, 50)	Slickenline (228, 15)	(342, 35)	(48, 16)	−29
(355, 64)	Slickenline (271, 12)	(8, 74)	(92, 22)	−23

Plus and minus values for pitch refer to clockwise and anticlockwise directions, respectively.

Japanese Islands (Takahashi and Saito, 1997). Next, tilting of the shear direction was corrected, which is due to the development of a map-scale synclinal fold with a west-plunging axis. The oceanic plate related to accretion of the Mino Belt is considered to be the Izanagi Plate, which subducted along the east side of the Asia Plate during the Jurassic-Cretaceous (Maruyama et al., 1997). Kimura (1999) suggests that the restored direction is subparallel to the plate motion of the

Table 2
Structural data from the asymmetric folds of bedded chert

Raw data		Restored data		
General bedding plane	Hinge line	Bedding plane	Shear direction	Pitch
(323, 89)	(235, 63)	(327, 76)	(35, 57)	−60
(330, 57)	(46, 21)	(355, 55)	(278, 18)	23
(320, 46)	(255, 24)	(358, 41)	(336, 39)	73
(320, 45)	(279, 37)	(359, 41)	(8, 41)	−84
(305, 42)	(223, 7)	(354, 31)	(302, 20)	42
(320, 62)	(230, 0)	(343, 53)	(288, 37)	49
(290, 50)	(305, 49)	(327, 27)	(25, 15)	−35
(285, 82)	(15, 3)	(293, 52)	(257, 46)	66
(277, 30)	(246, 26)	(19, 12)	(335, 9)	46
(300, 40)	(358, 24)	(354, 27)	(73, 5)	−11
(340, 40)	(255, 4)	(17, 48)	(323, 33)	47
(36, 56)	(306, 0)	(44, 85)	(327, 68)	68
(340, 62)	(250, 0)	(358, 64)	(297, 44)	51
(322, 77)	(236, 16)	(334, 66)	(295, 60)	71

Plus and minus values for pitch refer to clockwise and anticlockwise directions, respectively.

Izanagi Plate reconstructed by Engebretson et al. (1985) showing normal subduction under the Asia Plate during latest Jurassic to earliest Cretaceous times.

The imbricate stack in the Inuyama area is deformed as part of a west-plunging synclinal structure with a half-wavelength of 4 to 6 km. The coherent chert-basalt unit in the Takayama area has a similar synclinal structure to the imbricate stack in the Inuyama area. The tilting of the shear directions by this fold is corrected by restoring the west-plunging fold axis to horizontal. The fold axis trends S76°W and plunges 35°W, which follows the cylindrical best-fit of the poles of the bedding plane, based on the Bingham axes distribution calculated by use of StereonetPPC ver.6.0.2 (Allmendinger, 2001; Fig. 2b). In order to restore the shear directions to their position prior to tilting, they were rotated 35° clockwise with a horizontal axis facing N14°W. After the restoration, the shear directions from the shear zones in the siliceous claystones and basalts indicate dextral strike-slip to the east. In contrast, the restored shear directions from the asymmetric mesoscopic folds of the bedded chert indicate top-to-the south to southeast thrusting (Fig. 7).

The age of accretion of the coherent chert-basalt unit of the Takayama area is conceivably Jurassic, that is older than 145 Ma, according to the radiolarian age of the felsic tuff. Although relative plate motion of the Izanagi Plate in the Cretaceous from 85 to 145 Ma is reconstructed by Engebretson et al. (1985), the plate motion before 145 Ma is unknown. Therefore it is impossible at present to compare the shear directions derived from the field data in the Takayama area with the subducted plate motion reconstructed by paleomagnetic studies and hotspot track analyses. The shear zones in the siliceous claystones and basalts presumably correspond to the decollements, because the trend of the shear zones is subparallel to that of the slabs and clasts. However, it is difficult to correlate the restored dextral strike-slip direction of the shear zones in the siliceous claystones and basalts with the inferred direction of the subducted plate motion.

In order to interpret the formation of the dextral strike-slip shearing recorded in the siliceous claystones and basalts, we propose that the constituent rocks of the coherent chert-basalt unit in the Takayama area were obliquely subducted adjacent to the East Asian continental margin in Jurassic time (Fig. 8). When the oceanic plate is subducted dextrally oblique to the trench axis, shear on the oceanic plate initially reflects the direction of the offshore plate motion. As the plate is subducted, the deformation is subsequently partitioned into displacement components orthogonal and parallel to the trench axis in the onshore part (Fitch, 1972; Beck, 1983; Ellis and Watkinson, 1987; Platt et al., 1989; McCaffrey, 1993; Platt, 1993). Commonly, the trench-parallel shearing occurs contemporaneously with continued trench-orthogonal shearing (e.g. Northrup and Burchfiel, 1996; Davis et al., 1998).

One clear example of this process is illustrated by the present relationship between the Philippine Sea Plate and the Median Tectonic Line in Japan. The Philippine Sea Plate in the northwestern Pacific is subducting oblique to the Nankai Trough. Shear directions associated with deformation structures preserved in drill cores extracted from the Nankai Trough lie parallel to the plate motion of the Philippine Sea Plate, which shows the relatively early deformation in the offshore part (Byrne et al., 1993). For the onshore part, however, the deformation is partitioned into thrusting orthogonal to the Nankai Trough with dextral strike-slip shearing localized along the Median Tectonic Line (Fitch, 1972). Structural studies from older mountain chains also support the idea of strain partitioning (e.g. Ellis and Watkinson, 1987; Northrup and Burchfiel, 1996). Well-documented cases of strain partitioning during oblique convergence in ancient accretionary complexes are reported from several areas (e.g. Cashman et al., 1992; Davis et al., 1998; Holdsworth et al., 2002; Tavarnelli et al., 2004). Based on observations in more recent examples, this partitioning is most likely to occur in the deeper part of subduction zones.

Two distinct shear directions are preserved in the coherent chert-basalt unit of the Takayama area following restoration to remove the effects of later regional scale folding: (1) Thrusting of imbricate hanging walls of the imbricate thrust faults as recorded by shear directions deduced from mesoscopic asymmetric folding of bedded cherts either oblique or perpendicular to the trench axis along the Jurassic East Asian continental margin; and (2) Dextral strike-slip displacement shown by the slip direction of the shear zones in the siliceous claystones and basalts – this direction can be subparallel to the Jurassic trench axis. According to the deformation conditions, the mesoscopic asymmetric folding of the bedded chert probably occurred first in the shallower part of the subduction zone, i.e. during an earlier stage of accretion compared to the shearing in the siliceous claystones and basalts. Using a slip vector partitioning model, stage 1 is assigned to shearing subparallel to the plate motion in the earlier stage of the subduction process, whilst stage 2 is assigned to the trench-parallel shearing as a result of slip vector partitioning in the later stage. Trench-orthogonal shearing along the decollements in the siliceous claystones and basalts could have occurred initially in the coherent chert-basalt unit, but was subsequently overprinted by trench-parallel shearing localized in the weakened siliceous claystones and basalts.

In an earlier study of slip vector partitioning in accretionary complexes, Takagi (1999) suggested that strike-slip deformations could preferentially be accommodated by subvertical faults whereas thrust motions occur along moderate to low angle faults. Fig. 9 shows the relationship between dip angles of shear surfaces and pitch angles of shear directions in the siliceous claystones, basalts and bedded cherts. If the Takagi model is correct, slip direction data from the siliceous claystones and basalts should indicate low pitch angles and high dips, whilst slip direction data from the bedded cherts should indicate high pitch angles and low to moderate dips. This relationship is not clearly preserved and it therefore seems more likely that the different kinematic patterns are related to the depths at which the deformations occurred in subduction zone. Further studies are necessary to verify these relationships.

The model proposed here suggests that the Izanagi Plate was subducted dextrally oblique relative to the East Asian

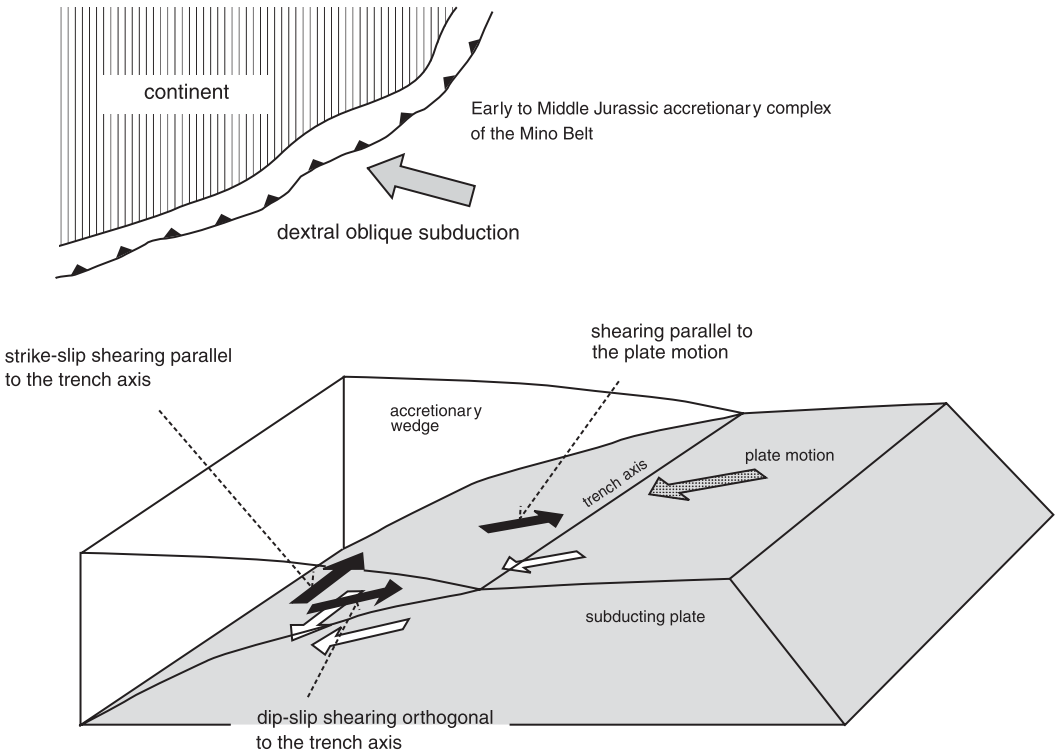

Fig. 8. Schematic model showing dextral oblique subduction along the continental margin of Jurassic East Asia. Black arrows = shear direction of hanging wall, white arrows = shear direction of footwall.

continental margin in Jurassic time. This suggestion differs significantly from previous studies of subducted plate motions, suggesting that a re-examination of the kinematics of late Mesozoic accretionary complexes in East Asia is needed.

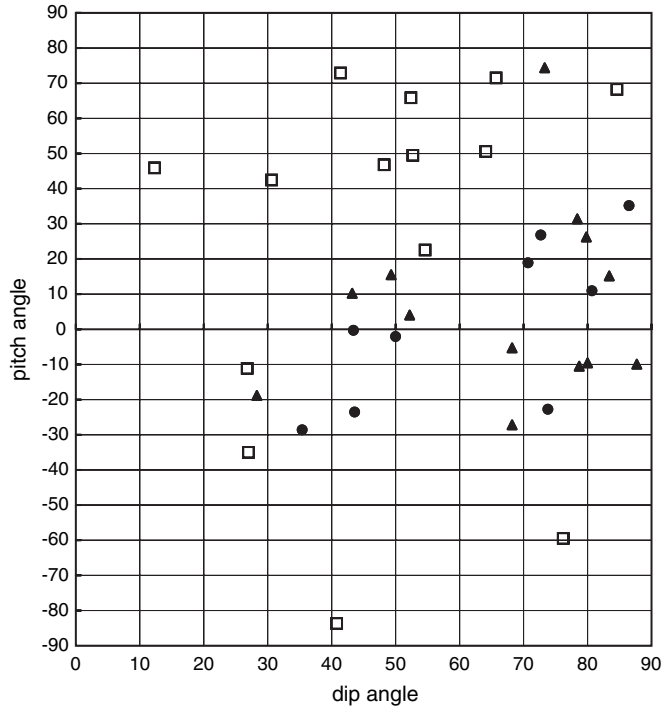

Fig. 9. Relationship between the dip angles of shear surfaces and pitch angles of shear directions after the restoration in the siliceous claystone (black triangle), basalts (black circle) and bedded chert (open square).

5. Conclusion

Deformation structures preserved in coherent chert-basalt unit in the Takayama area, Central Japan provide new insights into the accretion of oceanic rocks in the Jurassic. The main findings are as follows:

1. The coherent chert-basalt unit shows an imbricate structure composed of subparallel thrust sheets including abundant bedded cherts and basalts. Shear zones are developed in the siliceous claystones and basalts and are considered to most likely represent thrust sheet decollements. The sheared rocks include abundant phyllosilicates that show a strong alignment and define the foliation. Deformation structures in the shear zones are characterized by widespread evidence for the operation of diffusive mass transfer and cataclastic deformation mechanisms. The development of the shear zones suggests that the formation and presence of fine-grained phyllosilicate-rich units has led to preferential weakening localizing strain leading to the development of well-defined thrust sheet decollements.
2. Bedded cherts are affected by mesoscopic asymmetric folds. The folds are created by drag acting on the layering during subduction. The fold styles preserved suggest that the diagenesis of quartz influences the deformation of the cherts, and that the folds are likely to have preferentially formed under the P/T conditions corresponding to the opal-CT transformation. The folding of the bedded cherts appears to have occurred in a shallower part of

the subduction zones compared to the deeper level pressure solution-accommodated deformation observed in the siliceous claystones and basalts.

3. The slip directions are clearly different for the shear zones in the siliceous claystones and basalts, compared to the mesoscopic asymmetric folds in the bedded cherts. Following restoration of the regional west-plunging synclinal fold, a model is proposed in which the constituent rocks were subducted obliquely relative to the East Asian continental margin, with the slip vector was partitioned into two components in the deeper part of the subduction zone, one parallel and the other orthogonal to the trench axis. Thus, the asymmetric folds in the bedded cherts reflect shearing subparallel to the subducted plate motion in the shallower part of the subduction zone, while the shear zones in the siliceous claystones and basalts reflect a trench-parallel shearing due to slip vector partitioning in the deeper part.

Acknowledgements

I wish to thank Dr. K. Tsukada of Nagoya University for kind support and advice throughout the research. I also wish to thank Prof. M. Adachi, Associate Prof. M. Takeuchi, and Associate Prof. H. Yoshida of Nagoya University for helpful discussion and advice. I am indebted to Prof. S. Kojima of Gifu University and Prof. S. Otoh of Toyama University for valuable discussion. Associate Prof. S.R. Wallis of Nagoya University is thanked for reading the early draft. Mr. G. McCrank, an ex-JNC International Fellow, helped with the English. The constructive reviews by Prof. H. Takagi and Prof. T. Kusky, and editorial revisions by Prof. B. Holdsworth led to an improved paper, and are gratefully acknowledged. Part of this research was supported by Research Fellowships of the Japan Society for the Promotion of Science for Young Scientists (Grant no. 16005752).

References

Adachi, M., Kojima, S., 1983. Geology of the Mt. Hikagedaira area, east of Takayama, Gifu Prefecture, central Japan. The Journal of Earth Sciences, Nagoya University 31, 37–67.

Allmendinger, R.W., 2001. StereonetPPC ver.6.0.2 Academic version.

Beck Jr., M.E., 1983. On the mechanism of tectonic transport in zones of oblique subduction. Tectonophysics 93, 1–11.

Behl R.J., Garrison R.E., 1994. The origin of chert in the Monterey Formation of California (USA). International Geological Congress 29th Proceeding Part C, 101–132.

Bettelli, G., Vannucchi, P., 2003. Structural style of the offscraped Ligurian oceanic sequences of the Northern Apennines: new hypothesis concerning the development of mélange block-in-matrix fabric. Journal of Structural Geology 25, 371–388.

Bos, B., Spiers, C.J., 2001. Experimental investigation into the microstructural and mechanical evolution of phyllosilicates-bearing fault rock under conditions favouring pressure solution. Journal of Structural Geology 23, 1187–1202.

Bos, B., Spiers, C.J., 2002. Frictional-viscous flow of phyllosilicate-bearing fault rock: Microphysical model and implications for crustal strength profiles. Journal of Geophysical Research 107, doi:10.1029/2001JB000301.

Brueckner, H.K., Snyder, W.S., 1985. Structure of the Havallah sequence, Golconda allochthon, Nevada: Evidence for prolonged evolution in an accretionary prism. Geological Society of America Bulletin 96, 1113–1130.

Brueckner, H.K., Snyder, W.S., Boudreau, M., 1987. Diagenetic controls on the structural evolution of siliceous sediments in the Golconda allochthon, Nevada, U.S.A. Journal of Structural Geology 9, 403–417.

Byrne, T., Brückmann, W., Owens, W., Lallemant, S., Maltman, A., 1993. Structural synthesis: Correlation of structural fabrics, velocity anisotropy, and magnetic susceptibility data. Proceeding of the Ocean Drilling Program, Scientific Results 131, 365–378.

Cashman, S.M., Kelsey, H.M., Erdman, C.F., Cutten, H.N.C., Berryman, K.R., 1992. Strain partitioning between structural domains in the forearc of the Hikurangi subduction zone, New Zealand. Tectonics 11, 242–257.

Collettini, C., Holdsworth, R.E., 2004. Fault zone weakening and character of slip along low-angle normal faults: insights from the Zuccale fault, Elba, Italy. Journal of the Geological Society, London 161, 1039–1051.

Cowan, D.S., 1985. Structural styles in Mesozoic and Cenozoic mélanges in the western Cordillera of North America. Geological Society of America Bulletin 96, 451–462.

Davis, J.S., Roeske, S.M., Karl, S.M., 1998. Late Cretaceous to Early Tertiary transtension and strain partitioning in the Chugach accretionary complex, SE Alaska. Journal of Structural Geology 20, 639–654.

DiTullio, L., Byrne, T., 1990. Deformation paths in the shallow levels of an accretionary prism: The Eocene Shimanto belt of southwest Japan. Geological Society of America Bulletin 102, 1420–1438.

Ellis, M., Watkinson, A.J., 1987. Orogen-parallel extension and oblique tectonics: The relation between stretching lineations and relative plate motions. Geology 15, 1022–1026.

Engebretson, D.C., Cox, A., Gordon, R.G., 1985. Relative motions between oceanic and continental plates in the Pacific Basin. Geological Society of America Special Paper 206, 1–59.

Farver, J.R., Yund, R.A., 1999. Oxygen bilk diffusion measurements and TEM characterizations of a natural ultramylonite: implications for fluid transport in mica-bearing rocks. Journal of Metamorphic Geology 17, 669–683.

Fisher, D., Byrne, T., 1992. Strain variations in an ancient accretionary complex: Implications for forearc evolution. Tectonics 11, 330–347.

Fitch, T.J., 1972. Plate convergence, transcurrent faults, and internal deformation adjacent to Southeast Asia and the Western Pacific. Journal of Geophysical Research 77, 4432–4460.

Holdsworth, R.E., Tavarnelli, E., Clegg, P., Pinheiro, R.V.L., Jones, R.R., McCaffrey, K.J.W., 2002. Domainal deformation patterns and strain partitioning during transpression: an example from the Southern Uplands terrane, Scotland. Journal of the Geological Society, London 159, 401–415.

Imazato, A., Otoh, S., 1993. Jurassic radiolarians from the Nyukawa area, Northernmost part of the Mino Belt. News of Osaka Micropaleontologists Special Volume 9, 131–141 (in Japanese with English Abstract).

Imoto, N., 1984. Late Paleozoic and Mesozoic cherts in the Tamba Belt. southwest Japan (part 1). Bulletin of Kyoto University of Education Series B 65, 15–40.

Isozaki, Y., 1996. Anatomy and genesis of a subduction-related orogen: A new view of geotectonic subdivision and evolution of the Japanese Islands. The Island Arc 5, 289–320.

Isozaki, Y., 1997a. Jurassic accretion tectonics of Japan. The Island Arc 6, 25–61.

Isozaki, Y., 1997b. Permo-Triassic boundary superanoxia and stratified superocean: Records from lost deep sea. Science 276, 235–238.

Janecke, S.U., Evans, J.P., 1988. Feldspar-influenced rock rheologies. Geology 16, 1064–1067.

Jefferies, S.P., Holdsworth, R.E., Wibberley, C.A.J., Shimamoto, T., Spiers, C.J., Niemeijer, A.R., Lloyd, G.E., 2006. The nature and importance of phyllonite development in crustal-scale fault cores: an example from the Median Tectonic Line, Japan. Journal of Structural Geology 28, 220–235.

Jolivet, L., Takami, K., Fournier, M., 1994. Japan Sea opening history and mechanism: a synthesis. Journal of Geophysical Research 99, 22237–22259.

Kano, K., Konishi, Y., 2001. Deformation process in the shallow levels of an accretionary prism: The Mesozoic Torlesse Terrane, South Island, New Zealand. The Island Arc 10, 158–174.

Kano, K., Kosaka, K., Murata, A., Yanai, S., 1990. Intra-arc deformations with vertical rotation axes: the case of the pre-Middle Miocene terranes of Southwest Japan. Tectonophysics 176, 333–354.

Kimura, K., 1997. Offscraping, underplating and out-of-sequence thrusting process of an accretionary prism: On-land example from the Mino-Tamba Belt, central Japan. Bulletin of the Geological Survey of Japan 48, 313–337.

Kimura, K., 1999. The slip direction of thrust faults – A case study from a chert-clastic sequence in the Mino-Tamba Belt, central Japan. Journal of Geological Society of Japan 105, 208–226 (in Japanese with English Abstract).

Kimura, K., Hori, R., 1993. Offscraping accretion of Jurassic chert-clastic complexes in the Mino-Tamba Belt, central Japan. Journal of Structural Geology 15, 145–161.

Kimura, G., Ludden, J., 1995. Peeling oceanic crust in subduction zones. Geology 23, 217–220.

Kimura, G., Mukai, A., 1991. Underplated units in an accretionary complex: melange of the Shimanto Belt of eastern Shikoku, southwest Japan. Tectonics 10, 31–50.

Kojima, S., 1982. Some Jurassic, Triassic and Permian radiolarians from the eastern part of Takayama City, central Japan. News of Osaka Micropaleontologists Special Volume 5, 81–91 (in Japanese with English Abstract).

Kojima, S., 1984. Paleozoic-Mesozoic strata in the Takayama area, Gifu Prefecture, central Japan: their stratigraphy and structure. Journal of Geological Society of Japan 90, 175–190 (in Japanese with English Abstract).

Kusky, T.M., Bradley, D.C., 1999. Kinematic analysis of mélange fabrics: examples and applications from the McHugh Complex, Kenai Peninsula, Alaska. Journal of Structural Geology 21, 1773–1796.

Kusky, T.M., Young, C.P., 1999. Emplacement of the Resurrection Peninsula ophiolite in the southern Alaska forearc during a ridge-trench encounter. Journal of Geophysical Research 104, 29025–29054.

Kusky, T.M., Bradley, D.C., Haeussler, P.J., Karl, S., 1997. Controls on accretion of flysch and mélange belts at convergent margins: Evidence from the Chugach Bay thrust and Iceworm mélange, Chugach accretionary wedge, Alaska. Tectonics 16, 855–878.

Kusky, T.M., Ganley, R., Lytwyn, J., Polat, A.A., 2004. The Resurrection Peninsula ophiolite, mélange and accreted flysch belts of southern Alaska as an analog for trench-forearc systems in Precambrian orogens. In: Kusky, T.M. (Ed.), Precambrian Ophiolites and Related Rocks. Developments in Precambrian Geology 13. Elsevier, Amsterdam. pp. 627–674.

Labaume, P., Maltman, A.J., Bolton, A., Tessier, D., Ogawa, Y., Takizawa, S., 1997. Scaly fabrics in sheared clays from the decollement zone of the Barbados accretionary prism. Proceedings of the Ocean Drilling Program, Scientific Results 156, 59–77.

Liou, J.G., Maruyama, S., Cho, M., 1987. Very low-grade metamorphism of volcanic and volcaniclastic rocks-mineral assemblages and mineral facies. In: Frey, M. (Ed.), Low Temperature Metamorphism. Blackie and Son Ltd, Glasgow, pp. 59–113.

Logan, J.M., Friedman, M., Higgs, H.G., Dengo, C., Shimamoto, T., 1979. Experimental studies of simulated gouge and their application to studies of natural fault zones. In: Proceedings of Conference VIII – Analysis of Actual Fault Zones in Bedrock. U.S. Geological Survey Open-File Report 79–1239, 305–343.

Maltman, A.J., Byrne, T., Karig, D.E., Lallemant, S., Knipe, R., Prior, D., 1993. Deformation structures at site 808, Nankai accretionary prism, Japan. Proceedings of the Ocean Drilling Program, Scientific Results 131, 123–133.

Maruyama, S., Isozaki, Y., Kimura, G., Terabayashi, M., 1997. Paleogeographic maps of the Japanese Islands: Plate tectonic synthesis from 750 Ma to the present. The Island Arc 6, 121–142.

Matsuda, T., Isozaki, Y., 1991. Well-documented travel history of Mesozoic pelagic chert in Japan: From remote ocean to subduction zone. Tectonics 10, 475–499.

McCaffrey, R., 1993. On the role of the upper plate in great subduction zone earthquakes. Journal of Geophysical Research 98, 11953–11966.

Means, W.D., Williams, P.F., 1972. Crenulation cleavage and faulting in an artificial salt-silica schist. Journal of Geology 80, 569–591.

Moore, J.C., Allwardt, A., 1980. Progressive deformation of a Tertiary trench slope, Kodiak Islands, Alaska. Journal of Geophysical Research 85, 4741–4756.

Moore, J.C., Saffer, D., 2001. Updip limit of the seismogenic zone beneath the accretionary prism of southwest Japan: An effect of diagenetic to low-grade metamorphic process and increasing effective stress. Geology 29, 183–186.

Nakae, S., 1993. Jurassic accretionary complex of the Tamba Terrane, southwest Japan, and its formative process. Journal of Geosciences, Osaka City University 36, 15–70.

Nakae, S., 2000. Regional correlation of the Jurassic accretionary complex in the Inner Zone of Southwest Japan. Memoirs of Geological Society of Japan 55, 73–98 (in Japanese with English Abstract).

Niwa, M., 2004. Lithology, structure and correlation of the Hirayu Complex in the Mino Belt of the Takayama area, Gifu Prefecture, central Japan. Journal of Geological Society of Japan 110, 439–451 (in Japanese with English Abstract).

Northrup, C.J., Burchfiel, B.C., 1996. Orogen-parallel transport and vertical partitioning of strain during oblique collision, Efjorden, north Norway. Journal of Structural Geology 18, 1231–1244.

Okamura, Y., 1991. Large-scale melange formation due to seamount subduction: an example from the Mesozoic accretionary complex in central Japan. Journal of Geology 99, 661–674.

Orange, D.L., 1990. Criteria helpful recognizing shear-zone and diapiric mélanges: Examples from the Hoh accretionary complex, Olympic Peninsula, Washington. Geological Society of America Bulletin 102, 935–951.

Otofuji, Y., Matsuda, T., Nohda, S., 1985. Paleomagnetic evidence for the Miocene counter-clockwise rotation of Northeast Japan-rifting process of the Japan Arc. Earth and Planetary Science Letter 75, 265–277.

Otsuka, T., 1988. Paleozoic-Mesozoic sedimentary complex in the eastern Mino terrane, central Japan and its Jurassic tectonism. Journal of Geosciences, Osaka City University 31, 63–122.

Otsuka, T., 1989. Mesoscopic folds of chert in Triassic-Jurassic chert-clastics sequence in the Mino terrane, central Japan. Journal of Geological Society of Japan 95, 97–111.

Passchier, C.W., Trouw, R.A.J., 1996. Microtectonics. Springer, Berlin, p. 289.

Pini, G.A., 1999. Tectonosomes and oliststromes in the argille scagliose of the Northern Apennines, Italy. Geological Society of America Special Paper 335, 1–70.

Platt, J.P., 1993. Mechanics of oblique convergence. Journal of Geophysical Research 98, 16239–16256.

Platt, J.P., Leggett, J.K., Alam, S., 1988. Slip vectors and fault mechanics in the Makran accretionary wedge, southwest Pakistan. Journal of Geophysical Research 93, 7955–7973.

Platt, J.P., Behrmann, J.H., Cunningham, P.C., Dewey, J.F., Helman, M., Parish, M., Shepley, M.G., Wallis, S., Weston, P.J., 1989. Kinematics of the Alpine arc and the motion history of Adria. Nature 337, 158–161.

Renard, F., Ortoleva, P., Gratier, J.P., 1997. Pressure solution in sandstones: influence of clays and dependence on temperature and stress. Tectonophysics 280, 257–266.

Rutter, E.H., Maddock, R.H., Hall, S.H., White, S.H., 1986. Comparative microstructures of natural and experimentally produced clay-bearing fault gouges. Pure and Applied Geophysics 124, 3–30.

Sample, J.C., Moore, J.C., 1987. Structural style and kinematics of an underplated slate belt, Kodiak and adjacent islands, Alaska. Geological Society of America Bulletin 99, 7–20.

Suzuki, N., Ishida, K., Shinomiya, Y., Ishiga, H., 1998. High productivity in the earliest Triassic ocean: Black shales, Southwest Japan. Palaeogeography, Palaeoclimatology, Palaeoecology 141, 53–65.

Takagi, H., 1996. Foliated fault gouges. In: Snoke, A.W., Tullis, J., Todd, V.R. (Eds.), Fault-related Rocks: a Photographic Atlas. Princeton University Press, Princeton, pp. 58–61.

Takagi, H., 1999. Partitioning tectonics: Kinematic partitioning of strike-slip and thrust faulting (or folding) at transpression zones. Structural Geology 43, 21–31 (in Japanese with English Abstract).

Takahashi, M., Saito, K., 1997. Miocene intra-arc bending at an arc-arc collision zone, central Japan. The Island Arc 6, 168–182.

Tavarnelli, E., Holdsworth, R.E., Clegg, P., Jones, R.R., McCaffrey, K.J.W., 2004. The anatomy and evolution of a transpressional imbricate zone, Southern Uplands, Scotland. Journal of Structural Geology 26, 1341–1360.

Ueda, H., Kawamura, M., Niida, K., 2000. Accretion and tectonic erosion processes revealed by the mode of occurrence and geochemistry of greenstones in the Cretaceous accretionary complexes of the Idonnappu Zone, southern central Hokkaido, Japan. The Island Arc 9, 237–257.

Ujiie, K., 2002. Evolution and kinematics of an ancient decollement zone, mélange in the Shimanto accretionary complex of Okinawa Island, Ryukyu Arc. Journal of Structural Geology 24, 937–952.

Wakita, K., 1988. Origin of chaotically mixed rock bodies in the Early Jurassic to Early Cretaceous sedimentary complex of the Mino terrane, central Japan. Bulletin of Geological Survey of Japan 39, 675–757.

Wakita, K., Metcalfe, I., 2005. Ocean Plate Stratigraphy in East and Southeast Asia. Journal of Asian Earth Sciences 24, 679–702.

Williams, L.A., Crerar, D.A., 1985. Silica diagenesis, II. General mechanics. Journal of Sedimentary Petrology 55, 312–321.

Williams, L.A., Parks, G.A., Crerar, D.A., 1985. Silica diagenesis, I. Solubility controls. Journal of Sedimentary Petrology 55, 301–311.

Wintsch, R.P., Christoffersen, R., Kronenberg, A.K., 1995. Fluid-rock reaction weakening of fault zones. Journal of Geophysical Research 100, 13021–13032.

Yamada, N., Adachi, M., Kajita, S., Harayama, S., Yamazaki, H., Bunno, M., 1985. Geology of the Takayama district. Quadrangle Series, scale 1:50,000. Geological Survey of Japan (in Japanese with English Abstract).